PHYSICAL REVIEW A VOLUME 3, NUMBER 4 APRIL 1971

Experimental Rate Coefficients for Collisional Excitation of Lithiumlike Ions*

H.-J. Kunze and W. D. Johnston III
Department of Physics and Astronomy, University of Maryland, College Park, Maryland 20742
(Received 16 September 1970; revised manuscript received 19 November 1970)

Collisional excitation rates in N V, O VI, and Ne VIII have been derived from absolute line intensities emitted by these ions in a well-diagnosed plasma. The plasma was produced in a θ-pinch device, and several plasma conditions were investigated. The electron density and temperature were obtained as a function of radius and time from the spectrum of scattered laser light. The experimental results are compared with Bely's calculations using the Coulomb-Born approximation. Although the maximum error of the individual rate coefficients is a factor of 2, the standard deviation of the experimental values from the theoretical ones is less than 30% for excitation to the $n=2$ and $n=3$ levels and less than 40% for excitation to the $4s$ level. The rates to the $4p$ and $4d$ levels are on the average $\sim 60\%$ of the theoretical ones.

I. INTRODUCTION

Excitation-rate coefficients for ions of the lithium isoelectronic sequence are of considerable importance in the spectroscopy of laboratory as well as astrophysical plasmas. In 1963 Heroux[1,2] showed that the intensity ratio of the $2s$-$2p$ and $2s$-$3p$ transitions in the same lithiumlike ion allows a unique determination of the electron temperature as long as the plasma is optically thin and collisional depopulation can be neglected. Under these conditions the absolute intensities of the lines are controlled by collisional population rates from the ground state. In the laboratory this technique has been applied to numerous plasmas. Hinteregger *et al.*[3] used it to obtain temperatures from solar emission lines. Lines of lithiumlike ions are quite prominent in the solar spectrum, and their absolute intensities are conveniently used to deduce relative abundances of the various species.[4]

The study of lithiumlike ions is further intriguing from a theoretical point of view. Their simple electronic structure renders them amenable to rather detailed calculations (see Sec. II). A comparison of theoretical and experimental data is thus possible.

Direct measurements of the electron-impact excitation cross sections for multiply ionized atoms are very difficult. However, it is quite possible to measure the rate coefficients (i.e., the product of cross section and initial electron velocity averaged over the electron-velocity distribution function) in transient plasmas.[5-9] Atoms of interest are introduced into a well-diagnosed plasma and absolute line intensities are then interpreted in terms of desired rate coefficients.

II. THEORY

A. Principle of the Measurements

In a plasma which is optically thin with respect to the line radiation of interest, the emission coefficient of a spectral line arising from a spontaneous transition between bound levels p and q is given, per unit volume and per steradian, by

$$\epsilon(q,p) = (4\pi)^{-1} h\nu(q,p) A(q,p) N(p), \tag{1}$$

where $\nu(q,p)$ is the frequency of the emitted radiation, $A(q,p)$ is the atomic transition probability, and $N(p)$ is the population density of the upper level. At low electron densities N (i.e., neglecting cascading), the steady-state population[10] of the excited levels is determined by a balance between the sum of collisional excitation rates into that state and the sum of all spontaneous radiative decay rates. Lithiumlike ions have the further advantage that they have no metastable levels; at low electron densities, excitation occurs thus mainly from the ground state g, and the emission coefficient may be written

$$\epsilon(q,p) = \frac{h\nu(q,p)}{4\pi} \left(A(q,p) \Big/ \sum_{r<p} A(r,p) \right) \times NX(p,g) N(g) \ , \tag{2}$$

where $X(p,g)$ is the rate coefficient for excitation from the ground state.

In the actual experiment the determination of the ground-state population $N(g)$ of the ion of interest poses a most serious problem. At present there exists no direct way for its determination. The method usually employed, therefore, is to add the atoms of interest in small quantities to the filling gas and to assume that the mixing ratio and composition do not change during the discharge. One further has to know the fraction which is in the appropriate ionization stage. In steady-state plasmas this fraction can be calculated using the coro-

nal-equilibrium relationship. While the distribution of the ions in this model is independent of the electron density, it depends strongly on the magnitude of the collisional ionization and the radiative recombination coefficients. Unfortunately, these are not known with sufficient accuracy. However, in transient hot plasmas the degree of ionization lags behind the coronal-equilibrium situation: Each ion goes through successive ionization stages with a lifetime in each stage determined only by the ionization rates. (Recombination rates are usually very much smaller.) The rate equations governing the population in the various ionization stages are thus very much simplified.

Using the experimentally obtained electron temperature and density time histories, these equations can be solved numerically. It turns out that the peak population in each ionization stage depends less critically on the accurate value of the ionization rates than in the equilibrium situation. Thus estimates of the ground-state populations of the various ions are found with sufficient accuracy. With the emission coefficient $\epsilon(q,p)$ measured experimentally, Eq. (2) yields then the desired rate coefficient at the temperature existing in the plasma.

B. Theoretical Rate Coefficients for Excitation

Where no specific calculations are available the cross sections and rate coefficients for excitation of allowed dipole transitions are usually derived using the well-known $\bar{g}$ approximation of Seaton[11] and Van Regemorter.[12] They used the Bethe-Born approximation in the calculation of the cross sections, substituting, however, an effective Gaunt factor $\bar{g}$ which they determined empirically from all available cross-section data. In this approximation the rate coefficient can be written

$$X(p,q) = 1.60\times10^{-5}\,[f_{pq}\langle\bar{g}\rangle/\Delta E(kT)^{1/2}]\,e^{-\Delta E/kT}\ \mathrm{cm^3\,sec^{-1}}\,, \qquad (3)$$

where f_{pq} is the absorption oscillator strength, ΔE the energy difference between levels p and q, and kT the electron temperature, both measured in electron volts. The effective Gaunt factor $\langle\bar{g}\rangle$ averaged over a Maxwellian velocity distribution is given in Ref. 12 and can also be found in Ref. 13. Seaton and Van Regemorter's $\bar{g}$ is a function only of $E_i/\Delta E$, where E_i is the energy of the incident electrons. When deriving $\bar{g}$ from the quasiclassical line-broadening theory, Griem[14] suggested an additional dependence on two parameters, namely, the Coulomb parameter and the relative size of the dipole matrix elements. This dependence, however, is weak. Work along similar lines has also been done by Roberts.[15]

For the collisional excitation by (optically forbidden) monopole or quadrupole transitions, a corresponding approximate formula does not exist. An order of magnitude estimate can be obtained through the collision strength (see, e.g., Refs. 13 and 16).

Recently, cross sections have been calculated specifically for ions of the lithium-isoelectronic sequence. Burke *et al.*[17] computed the excitation cross sections corresponding to the array $2s$, $2p$, $3s$, $3p$, $3d$ in N v using both the Coulomb-Born and the close-coupling methods, while Bely[18–20] did the calculations for the transitions $2s\rightarrow ns$, $2s\rightarrow np$, and $2s\rightarrow nd$ as well as $2p\rightarrow ns$, $2p\rightarrow np$, and $2p\rightarrow nd$ for Be II, N v, Ne VIII, and for a hydrogenic ion with an infinite nuclear charge using only the Coulomb-Born approximation. The conclusions and results of both calculations are essentially the same, where they overlap. Bely's results are given in a form convenient for extrapolation to other ions and higher principal quantum numbers, so they will be used in the following. He was able to fit the computed cross sections to an analytical form; this allows a convenient integration over the velocity distribution in order to obtain the rate coefficients. Figure 1 shows these rate coefficients for the excitation from the ground state to the $2p$, $3p$, and $4p$ levels in N v, O VI, and Ne VIII. Figure 2 compares the $2s$-$3s$, $2s$-$3p$, and $2s$-$3d$ excitation rates for N v and Ne VIII. At low electron temperatures (near threshold), the quadrupole and monopole excitation are found to be much larger than the dipole excitation. At higher temperatures all excitation rates are, roughly speaking, comparable, though the quadrupole transition remains the strongest one. According

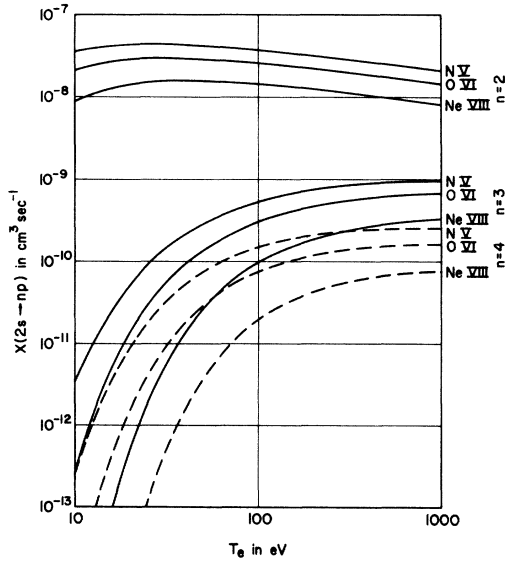

FIG. 1. Excitation-rate coefficients, after Bely, as a function of electron temperature for the transitions $2s\rightarrow np$ with $n=2,3,4$ in N v, O VI, and Ne VIII.

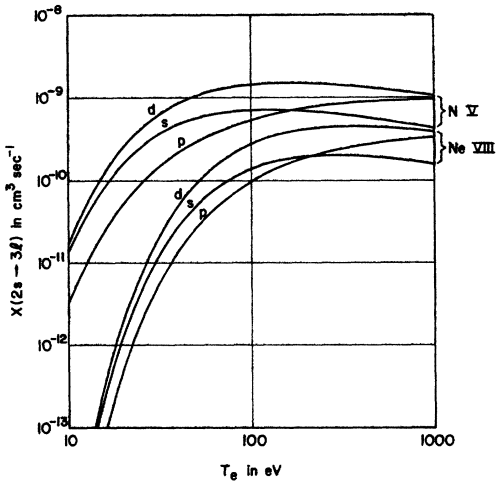

FIG. 2. Excitation-rate coefficients, after Bely, as a function of electron temperature for the transitions $2s \rightarrow 3l$ with $l = s, p, d$ in N v and Ne VIII.

to the author[18,19] the values shown in the curves above should be good to about 20% for the $2s$-$2p$ transitions and to better than 50% for all the other transitions. We should mention, however, that the author calculated the cross sections only to five and ten times the threshold energy, respectively, so that the excitation coefficients (Figs. 1 and 2) at high temperatures depend somewhat on the analytical form of the cross section adopted by Bely,[18] which is correct only for dipole transitions. Further, it is interesting to note that by far the strongest rates in lithiumlike ions are those for the $2p$-nd transitions.

III. EXPERIMENT

A. Apparatus

The plasma used for these experiments was produced in a θ-pinch machine described in detail elsewhere.[21] The measurements being discussed were done mainly with an energy of 15 kJ stored in the main bank, although some results were also obtained with the original 9-kJ version. The energy in the preheater was slightly increased; also increased was the damping of the preheater discharge in order that the main discharge could be fired 15 μsec after the preheater. The filling gas was always hydrogen, and the elements of interest (nitrogen, oxygen, and neon) were added in small quantities ($< 1\%$). As pointed out in Sec. I, one basic assumption for our measurements is that the mixing ratio does not change during the discharge. This assumption is supported by the fact that, when adding known amounts of the impurities, line intensities observed from various ionization stages were found to increase linearly,[22] which excludes nonlinear wall effects. The C v 2271-Å line viewed radially at the midplane of the coil was used again as the monitor of the plasma conditions.

Several discharge conditions were investigated. They were obtained by varying the energy stored in the main bank, the filling pressure, the magnitude of the bias magnetic field, and the time between the beginning of the preheater discharge and the ignition of the main bank.

B. Determination of Plasma Parameters

The electron density and temperature were derived as functions of radius and time from the analysis of laser light scattered by the plasma. A general description of this technique can be found, e.g., in Ref. 23. The specific setup is identical to that used in Ref. 9, and the whole experimental arrangement can be seen in Fig. 3. Laser head and multichannel detection system are mounted on a common carriage, thus permitting easy scanning of the scattering volume along a diameter of the plasma column in the midplane of the coil. Results for two cases are shown in Refs. 9 and 24. For quantitative spectroscopic observations one needs the length of the hot plasma core. This was determined by observing the C v 2271-Å line through equidistant holes in the coil. The length changed with time, and at the time of maximum compression it varied between 8 and 15 cm for the different discharge conditions.

C. Absolute Sensitivity Calibration of Two Vacuum Ultraviolet Monochromators

The lines of interest from lithiumlike ions are in the vacuum uv wavelength region. Two monochromators were used for their measurement: A 2-m grazing-incidence instrument (1200 lines per mm and a grazing-incidence angle of 86°) covered the wavelength region from 60–600 Å, while a normal incidence instrument of the Seya-Namioka-type mount was used for the wavelength region above 400 Å.

The most serious problem connected with the measurement of absolute line intensities in the vacuum uv region is that no reliable radiation standards are available. We employed, therefore, the "branching-ratio technique," which was developed by Griffin and McWhirter[25] and by Hinnov and Hofmann.[26] This technique is based on the observation of spectral lines in the vacuum uv and the visible regions, both of which originate from the same upper level and neither of which is affected by self-absorption. The intensity ratio (in photon units) of the two lines is then simply given by the ratio of the respective transition probabilities. The method can

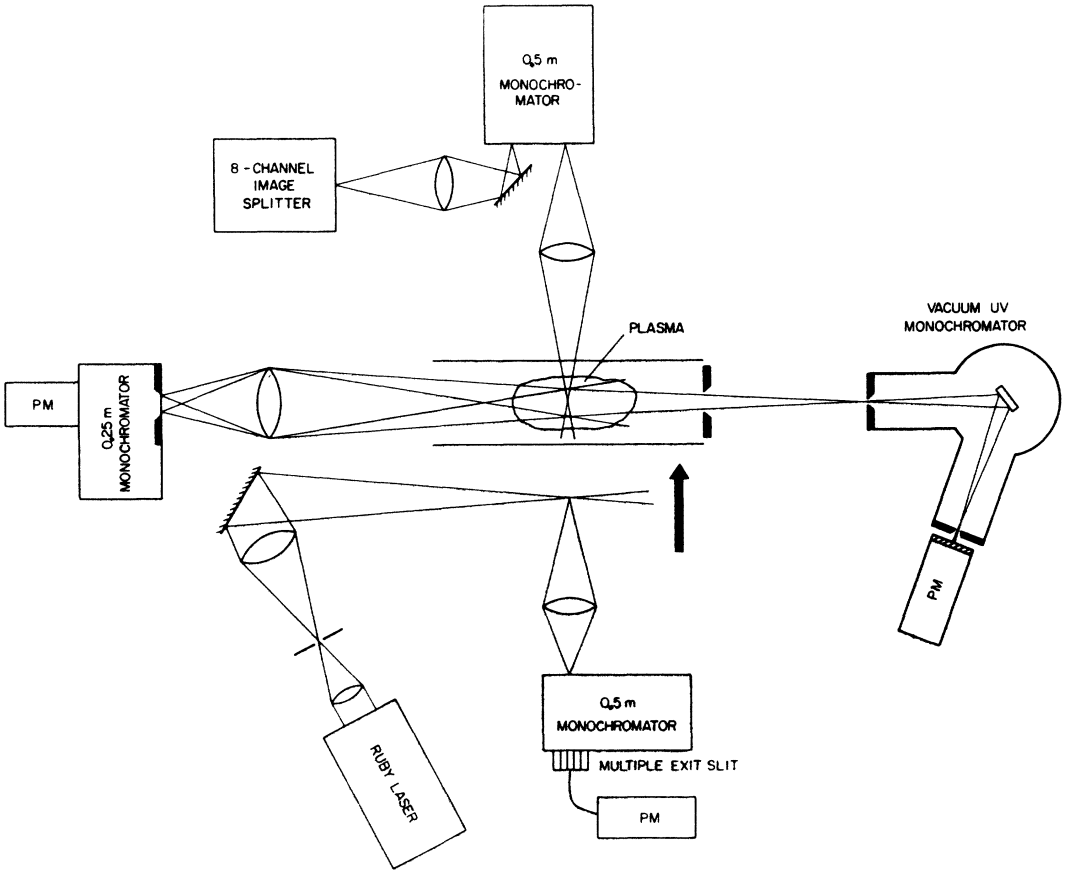

FIG. 3. Experimental arrangement.

be extended to lines which originate from different fine-structure sublevels if one can prove reliably that the sublevels are populated according to their statistical weights.

Both monochromators were equipped with photomultipliers at the exit slit; p-terphenyl as well as the plastic Pilot B were used as scintillators. The calibration was done *in situ*, and for this purpose an appropriate plasma was produced in the discharge tube. An aperture stop assured that during both situations, calibration and actual measurement, the field of view of the instruments was limited to 1.25 cm at the center of the discharge tube. During the calibration, the same plasma volume was imaged through the other end of the discharge tube onto the entrance slit of a 0.25-m visible monochromator, also equipped with a photomultiplier tube. This dual arrangement has the advantage that all geometrical factors canceled. The visible instrument was calibrated using both a tungsten lamp and a carbon arc.[27,28]

The line pairs used for the calibration of the two vacuum uv instruments are given in Table I. The wavelengths quoted, as well as the transition probabilities required for the calibration, were taken from Wiese *et al.*[29] with the exception of the wavelength of the $3s$-$3p$ transition in Ne VIII which is from Ref. 30.

For the calibration of the grazing-incidence instrument the $2s$-$3p$ and $3s$-$3p$ line pairs of the lithiumlike ions [Table I, lines (a)–(d)] are most suitable. Here, the transition probabilities should be accurate to better than 10%. The intensity ratios of the two lines of the $3s$-$3p$ doublets were found to be 2 in all cases, thus assuring equilibrium population between the two upper levels. The transition probabilities of the corresponding line pair in berylliumlike O V [Table I, line (e)] are much less accurate; however, the obtained calibration point falls right on the curve, suggesting that at least the ratio of the transition probabilities is reliable.

The calibration of the Seya-Namioka monochromator was more problematic since not too many suitable line pairs could be found covering the required wavelength region. We finally calibrated the instrument using the line pairs (f) to (k) of Table I.

In contrast to the calibration of the grazing-incidence instrument, where we used the same plasma under investigation also for calibration purposes, we now had to produce different plasmas in the dis-

TABLE I. Line pairs for branching-ratio calibration.

	Ion	λ(Å)	Transition	λ(Å)	Transition
(a)	C IV	312.4	$2s^2S_{1/2}-3p^2P_{1/2,3/2}$	5802	$3s^2S_{1/2}-3p^2P_{3/2}$
(b)	N V	209.3	$2s^2S_{1/2}-3p^2P_{1/2,3/2}$	4620	$3s^2S_{1/2}-3p^2P_{1/2}$
(c)	O VI	150.1	$2s^2S_{1/2}-3p^2P_{1/2,3/2}$	3811	$3s^2S_{1/2}-3p^2P_{3/2}$
(d)	Ne VIII	88.1	$2s^2S_{1/2}-3p^2P_{1/2,3/2}$	2860	$3s^2S_{1/2}-3p^2P_{1/2}$
(e)	O V	172.2	$2s^{21}S-2s3p^1P$	5114	$2s3s^1S-2s3p^1P$
(f)	He II	1215	n: 2 – 4	4686	n: 3 – 4
(g)	He II	1085	n: 2 – 5	3203	n: 3 – 5
(h)	H	1026	L_β	6563	H_α
(i)	C III	574.3	$2p^1P^0-3d^1D$	5696	$3p^1P^0-3d^1D$
(j)	He I	515.6	$1s^1S-5p^1P$	3614	$2s^1S-5p^1P$
(k)	H	972.5	L_γ	4861	H_β

charge tube, and we will comment on the difficulties encountered for each line pair. The calibration using the He II line pairs is, in principle, straightforward. For best results we produced a hot plasma with the main bank using an initial filling pressure of 70-mTorr He. However, attention has to be paid to the fact that the strong He II L_α line (304 Å) in fourth order, as well as spurious amounts of hydrogen (L_α line), can obscure the He II line at 1215 Å. At 1085 Å we also have the resonance lines of N II; spurious amounts of N II can thus falsify the result. We therefore always crosschecked the N II contribution by comparison with another line at 916 Å of the same multiplet.

The L_β-H_α line pair in hydrogen [Table I, line (h)] has to be used with caution because it is nearly impossible to produce a plasma in the laboratory where L_β is not affected by self-absorption, at least in cooler outer regions. The technique usually employed is, therefore, to decrease the density as far as possible and to extrapolate to the absorption-free limit.[31] This, however, can still be afflicted with relatively large uncertainties, and since it is also difficult to produce plasmas of sufficiently low density in a θ pinch, we modified the method and went to the other extreme. Using a helium-hydrogen mixture (95% helium, 5% hydrogen) at 2 Torr we produced a plasma having an electron density $N \approx 2 \times 10^{18}$ cm^{-3}. Both lines are now very broad, and their shape is determined by the Stark effect and by self-absorption. The self-absorption, however, affects the line profiles only in the center and not on the wings. Theoretical line profiles for hydrogen are known now to a high accuracy,[32,33] and a comparison of the intensities on the wings of the two lines can thus easily be related to the ratio of their total intensities. (Note that the intensity ratio of the wings should be of even higher accuracy than the individual line profiles, since uncertainties in the profiles due to approximations in their calculation will tend to cancel in the ratio.) The maximum error in the absolute calibration for these 3 points will be 20% or less.

The C III line pair poses no experimental problem at low electron densities. Here the drawback is, at present, the large uncertainty in the theoretical transition probabilities.[29] The He I [Table I, line (j)] and H [Table I, line (k)] line pairs again will be influenced by self-absorption since both short-wavelength lines go to the ground state. For the L_λ-H_β ratio we used only the preheater discharge, decreased the density as much as possible, and extrapolated to zero density; in the case of the He I line pair we used a hot plasma (10-mTorr He filling pressure) at early times of the discharge. Due to Doppler shift and Doppler broadening, the reabsorption of the uv line in the cooler outer region should be thus decreased.

Three of the calibrations [Table I, lines (i)–(k)] could be afflicted, as discussed, with relatively large uncertainties. A higher degree of accuracy, however, is suggested by the following fact: If we take the known transmission curve of the monochromator[34] and assume constant quantum efficiency for the scintillator (p-terphenyl), we obtain a relative sensitivity curve which can be scaled to fit the obtained absolute calibration points. The maximum deviation of all six points from this sensitivity curve is found to be 30%, and this covers the wavelength region from 515–1215 Å.

D. Experimental Results

Table II shows the emission coefficients of the resonance lines obtained for the different ions under the various discharge conditions. The emission coefficients are given for each line at the time of their peak intensity and are reduced to an impurity concentration of 1% relative to the electron density N. (The actual quantity obtained is the intensity of the lines in W/cm^2 sr; it was divided by the length of the plasma column.) The $2s^2S$-$2p^2P$ transitions of the lithiumlike ions pose some difficulties inasmuch as they easily become optically thick. The line intensities were measured, therefore, for various impurity concentrations between 0.1 and 1.0% and were extrapolated, where neces-

TABLE II. $2s^2S-2p^2P$ radiative transitions.

Ion	Transition	λ (Å)	$\epsilon(W/cm^3sr)$	N (cm^3)	T (eV)	p (%)
Ne VIII	$2s^2S-2p^2P_{3/2}$	770.4	112	4.5×10^{15}	260	46
			197	6.4×10^{15}	165	55
			236	6.9×10^{15}	125	56
O VI	$2s^2S-2p^2P_{3/2}$	1032	73	2.8×10^{15}	215	45
N V	$2s^2S-2p^2P_{1/2,3/2}$	1240	185	3.8×10^{15}	210	44
			306	4.9×10^{15}	145	44
			460	6.2×10^{15}	110	46
			118	2.8×10^{15}	215	44

sary, to the absorption-free limit. There were no problems for N V and Ne VIII, and the necessary corrections were usually less than 10%. For O VI, however, the situation was different. Oxygen is a natural contaminant in our plasma. Its concentration varies between 1.5 and 3% for the different discharge conditions; the resonance line of O VI was influenced, therefore, by self-absorption already without any addition of oxygen. Although the values obtained are less reliable, attempts were made to correct for the optical thickness theoretically.

As suggested in Ref. 8, a uniform plasma column much longer than its diameter may be considered as having a constant source function over the length viewed for the line radiation of interest. (In other words, this approximation assumes that the population of the upper level of the line of interest is nowhere substantially influenced by reabsorption of the line.) For this case the equation of radiative transfer can be solved and the spectral intensity of a line can be expressed in terms of the optical depth. Lines in high-temperature plasmas usually are broadened only by Doppler effect, which is shown experimentally by measuring the line profiles of appropriate lines. In this case the source function is even frequency independent, and the solution can be integrated and the total line intensity expressed in terms of the source function and optical depth τ_0 at the center of the Doppler-broadened line. If one compares this intensity with the intensity obtained if no absorption took place, the correction factor for the line intensity due to absorption is obtained. This factor is solely a function of the optical depth at the line center, and it is tabulated in Ref. 35. The optical depth at the line center can readily be calculated for our plasma conditions [see Ref. 32, Eqs. (8)–(14)]. The temperature of the O VI ions was taken to be equal to the measured temperature of the C V ions. In Table II we quote only the final value obtained with the lowest electron density; the correction which had to be applied in this case was 15%.

The fifth and sixth column of Table II give the electron density and temperature (for the same time); the last column shows the corresponding relative concentration p of the atom in the particular ionization stage obtained by solving the coupled rate equations using a computer program and matching calculated and observed time histories of spectral lines. Due to changing density and temperature, the time of the peak intensity of a line does not always coincide with that of the peak concentration of the ion.

At low impurity concentrations the two components of the doublet always show a 2:1 intensity ratio which corresponds to a population of the $2p^2P$ levels according to their statistical weights. For O VI, however, this was not the case, the ratio being smaller. This can be understood readily since the stronger line is much more influenced by self-absorption than the weaker one.

Tables III and IV give the corresponding results for lines from $n=3$ and $n=4$ levels, respectively. The fine-structure lines were not resolved, so the emission coefficient of the doublet is quoted. We also give the results for one oxygen case only, since at higher electron densities even the $3p\rightarrow 2s$ and $3d\rightarrow 2p$ transitions were influenced by self-absorption.

IV. INTERPRETATION AND DISCUSSION

A. Population Densities of Excited Levels

In the low-density limit the excitation-rate coefficients could now be calculated from the measured quantities using Eq. (2). However, at our electron densities this limit will not hold for all

TABLE III. Radiative transitions from $n=3$ levels.

	ϵ(W/cm^3sr)					
Ion	$2s$-$3p$	$2p$-$3s$	$2p$-$3d$	N(cm^3)	T(eV)	p(%)
Ne VIII	37	28	64	4.5×10^{15}	260	46
	75	53	151	6.4×10^{15}	165	55
	118	81	183	6.9×10^{15}	125	56
O VI	30	24	87	5.0×10^{15}	260	45
N V	45	22	87	3.8×10^{15}	210	44
	75	32	165	4.9×10^{15}	145	44
	124	46	279	6.2×10^{15}	110	46

TABLE IV. Radiative transitions from $n=4$ levels.

	ϵ(W/cm^{3}sr)					
Ion	$2s$-$4p$	$2p$-$4s$	$2p$-$4d$	N(cm^3)	T(eV)	p(%)
Ne VIII	6.5	4.2	7.4	4.5×10^{15}	260	46
	8.2	11.0	13.5	6.4×10^{15}	165	55
	13.5	12.8	20.4	6.9×10^{15}	125	56
O VI	6.4	2.5	9.2	5.0×10^{15}	260	45
N V	4.6	2.8	13.8	3.8×10^{15}	210	44
	7.7	4.6	19.4	4.9×10^{15}	145	44
	10.9	5.3	33	6.2×10^{15}	110	46

cases. At higher electron densities the population of the low-lying $2p$ level becomes considerable and thus also the excitation of higher levels from this $2p$ level. As a first step we calculate, therefore, the population densities $N(p)$ of all excited states from the measured emission coefficients using Eq. (1) and the transition probabilities as given in Refs. 29 and 36. These population densities of the excited states are then compared with the total concentration N_{tot} of each ionization stage as obtained from the solution of the rate equations. We have $N_{tot} = 10^{-4}pN$, since p is expressed in percent in Tables II–IV; the emission coefficients were reduced to an impurity concentration of 1% relative to the electron density N.

One obtains that the population of the $2p$ level is considerable. It varies from ~7% for Ne VIII to ~40% for N V for the highest-density case. The population of all $n=3$ levels is lower than 0.01% for Ne VIII and around 0.1% for the N V case mentioned above. The total population of all $n=4$ levels, finally, is about a factor of 3 below that of the $n=3$ levels. In the analysis of the emission coefficients it is justified, therefore, to neglect all ions in higher excited states, i.e., we assume that only the ground and the $2p^2P$ states are significantly populated.

B. Excitation to the $2p$ Level

In a first approximation we make the assumption that the population of the $2p^2P$ level is determined by a balance between collisional excitation from the ground state and radiative decay and collisional deexcitation to the ground state. The deexcitation rate is deduced from the excitation rate using the principle of detailed balance, $X(2p \to 2s) = \frac{1}{3}X(2s \to 2p)$. The rate coefficient can be derived then from the population of the $2p$ level and is given by

$$X(2s \to 2p) \simeq [N(2p)/N]A/[p10^{-4}N - \tfrac{4}{3}N(2p)] \quad . \quad (4)$$

The results obtained are given in Table V. In order to justify this assumption we also consider, as a second step, the depopulation of the $2p$ level by further excitation as well as a population by cascading from higher levels. This results in two additional terms in the rate equation for the population of the $2p$ level which we have to compare with each other as well as with the other rates used above. The cascading contribution is readily obtained from the measured emission coefficients. We consider only cascading from the $n=3$ levels, the cascading contribution from the $n=4$ levels being found to be smaller by a factor of ~10.

For Ne VIII the depopulation of the $2p$ level by further excitation is found to be about one-half the rate for collisional deexcitation to the ground state and only a few percent of the radiative decay rate. (Cross sections as given by Bely[20] were used for these estimates.) The population of the $2p$ level by cascading is less than 10% of the collisional excitation rate. Since, furthermore, both additional rates enter with opposite signs into the rate equation, they tend to cancel, and the total error introduced by neglecting them will be ~5%. Although ~40% of the N V ions are in the $2p^2P$ state of N V in the high-density case, the error introduced by neglecting cascading *and* further excitation is found to be ~5% also in this case.

C. Excitation to $n = 3$ Levels

When considering the population of the $n=3$ and $n=4$ levels the situation becomes more complicated insofar as at higher electron densities not only a strong population via the $2p^2P$ state occurs, but also the collisional rates between levels of the same principal quantum number become comparable to or even larger than the radiative rates: The levels would be populated then according to their statistical weights, and no individual excitation rates can be deduced any more.

We consider first the high-density N V case. The cross sections for collisional transitions between the $n=3$ levels have been calculated by Burke *et al.*[17] We average these cross sections over the Maxwellian velocity distribution and compare these rates with the radiative transition probabilities[29] from the $n=3$ levels. We find that the level most severely influenced by $n=3$ collisional transitions is the $3s$ level, the $3s \to 3p$ transition being 22% of

TABLE V. $2s \to 2p$ excitation-rate coefficients.

		$X(2s \to 2p)$ (cm^{3}sec^{-1})		
Ion	T (eV)	Measured	Bely	Seaton, Regemorter
Ne VIII	260	1.0×10^{-8}	1.2×10^{-8}	0.6×10^{-8}
	165	0.7×10^{-8}	1.3×10^{-8}	0.6×10^{-8}
	125	0.7×10^{-8}	1.4×10^{-8}	0.6×10^{-8}
O VI	215	2.5×10^{-8}	2.2×10^{-8}	1.2×10^{-8}
N V	215	3.8×10^{-8}	3.1×10^{-8}	1.8×10^{-8}
	210	3.6×10^{-8}	3.2×10^{-8}	1.8×10^{-8}
	145	4.0×10^{-8}	3.4×10^{-8}	1.9×10^{-8}
	110	4.1×10^{-8}	3.7×10^{-8}	1.9×10^{-8}

the radiative decay. More than one-half of this population loss, however, is offset by collisional transitions in the opposite direction, so that the net drain of the $3s$ level by collisions to the $3p$ level is about 10% only. Similarly, the population of the $3d$ level occurs to about 10% through collisions from the $3p$ level. The population of the $3p$ level is practically not influenced by these collisions, the drain to the $3d$ level being nearly offset by the gain from the $3s$ level. For the lower electron densities the collisions between the $n=3$ levels become even less important. Naturally they can be neglected for higher Z ions, O VI and Ne VIII in our cases.

Very important, however, is the excitation of the $n=3$ levels via the $2p$ level. The steady-state population of any level is given now by

$$N(3l)A \simeq N(2s)NX(2s \rightarrow 3l) + N(2p)NX(2p \rightarrow 3l) . \quad (5)$$

We consider again, at first, the high-density N V case ($T_e = 110$ eV, $N = 6.2\times10^{15}$ cm^{-3}). Theoretical calculations[18–20] yield for the rate coefficients (in units cm^3 sec^{-1})

$$X(2s \rightarrow 3s) = 7.1\times10^{-10}, \quad X(2p \rightarrow 3s) = 1.6\times10^{-10},$$

$$X(2s \rightarrow 3p) = 5.6\times10^{-10}, \quad X(2p \rightarrow 3p) = 10.6\times10^{-10},$$

$$X(2s \rightarrow 3d) = 14.8\times10^{-10}, \quad X(2p \rightarrow 3d) = 49.4\times10^{-10},$$

and from the experiment one obtains

$$N(2s) = 1.78\times10^{13} \text{ cm}^{-3}, \quad N(2p) = 1.07\times10^{13} \text{ cm}^{-3} .$$

Theoretically, one obtains, in this case, that the population via the $2p$ level is 13% for the $3s$ level, 53% for the $3p$ level, and even 67% for the $3d$ level. (The corresponding values for Ne VIII, $T_e = 260$ eV, and $N = 4.5\times10^{15}$ cm^{-3}, are 1%, 8%, and 18%, respectively.) For all cases and ions it is thus possible to derive the $2s \rightarrow 3s$ excitation rate directly from the corresponding emission coefficient using, for example, Eq. (2); this is also still possible (with a small correction) for the rates to the $3p$ and $3d$ levels of Ne VIII. However, for N V one obtains, for $3p$ and $3d$, only rates averaged over the $2s$ and $2p$ levels.

For all theoretical excitation cross sections the Coulomb-Born approximation was used.[18–20] Since our average kinetic energies are at least three times above threshold, the relative magnitude of the theoretical cross sections from the $2s$ and $2p$ levels to the same upper level should be very reliable, even if the absolute values show larger uncertainties; approximations should influence both cross sections in the same way and will tend to cancel in the ratio. We accept, therefore, the theoretical ratio R of the two excitation rates (which is a function of T) of Refs. 18–20 and use it in the analysis of the data, i.e., we substitute $X(2p \rightarrow 3l) = RX(2s \rightarrow 3l)$ in Eq. (5). Table VI shows the rate coefficients thus obtained. They again are compared with the theoretical values. (For O VI the population of the $2p$ level was calculated using the theoretical rate since the resonance line was optically thick for the case quoted.)

In the final evaluation of the rate coefficients also the cascading contributions from the $n=4$ levels as derived from measured line intensities were taken into account. (For N V they were, for example, 4% for the $3s$ level, 7% for the $3p$ level, and ~7% for the $3d$ level, where the cascading from the $4f$ level could only be estimated.)

D. Excitation to $n = 4$ Levels

Collisions within the $n=4$ levels will influence the respective population densities more severely than within the $n=3$ levels. No theoretical calculations are available at present. Classical scaling suggests that the rates are larger by a factor of ~3 compared to those within the $n=3$ levels. Since the radiative rates are smaller by a factor of ~2, the ratios of collisional $n=4$ transitions to radiative decay rates are larger by a factor of ~6, as compared to the respective ratios for the $n=3$ levels. Individual excitation rates could thus be off by up to ~50% in the high-density N V case. However, these collisions still do not dominate the population densities, which can be seen from the experimentally obtained values. In the collision-dominated case one would find $N(4s) : N(4p) : N(4d) = 1 : 3 : 5$. Table VII shows the rate coefficients derived in the way as discussed in Sec. IV C. A 10% correction for cascading was applied in all cases.

E. Estimate of Accuracy

The maximum error for the individual rate coefficients is estimated to be a factor of 2 for excitation to the $n=2$ and $n=3$ levels, and less than a factor of 2.5 for excitation to the $n=4$ levels. The larger error in the latter cases is essentially due to the uncertainty in the collisional mixing of the $n=4$ levels.

Though all individual measurements are of relatively high accuracy, the large error in the final value of an individual rate coefficient is simply a consequence of the number of measurements which have to be done and of the assumptions needed for the evaluation. The uncertainty in the calibration of the grazing-incidence instrument is about 20%, of the Seya-Namioka monochromator about 30%. The electron density is estimated to be accurate to about 10%, the electron temperature to 10%, the length of the plasma column to 10%, the total concentration of the ions to 10%, the computed value p of the concentration of the ion in the specific ionization stage to 10%; the uncertainty introduced by optical-depth effects is about 5%, and that caused by insufficient correction for cascading from higher

TABLE VI. Excitation-rate coefficients to $n = 3$ levels.

Ion	Rate coefficient ($cm^3 sec^{-1}$)	T (eV)	Measured	Bely
Ne VIII	$X(2s \rightarrow 3s)$	125	1.9×10^{-10}	1.6×10^{-10}
		165	1.6×10^{-10}	1.9×10^{-10}
		260	2.0×10^{-10}	2.0×10^{-10}
	$X(2s \rightarrow 3p)$	125	2.0×10^{-10}	1.3×10^{-10}
		165	1.5×10^{-10}	1.6×10^{-10}
		260	1.9×10^{-10}	2.2×10^{-10}
	$X(2s \rightarrow 3d)$	125	3.4×10^{-10}	3.3×10^{-10}
		165	3.5×10^{-10}	4.0×10^{-10}
		260	3.4×10^{-10}	4.4×10^{-10}
O VI	$X(2s \rightarrow 3s)$	260	3.0×10^{-10}	4.3×10^{-10}
	$X(2s \rightarrow 3p) = 0.94X(2p \rightarrow 3p)$	260	2.5×10^{-10}	5.2×10^{-10}
	$X(2s \rightarrow 3d) = 0.33X(2p \rightarrow 3d)$	260	5.3×10^{-10}	9.5×10^{-10}
N V	$X(2s \rightarrow 3s)$	110	6.6×10^{-10}	7.1×10^{-10}
		145	6.7×10^{-10}	7.1×10^{-10}
		210	7.6×10^{-10}	6.8×10^{-10}
	$X(2s \rightarrow 3p) = 0.53X(2p \rightarrow 3p)$	110	6.3×10^{-10}	5.6×10^{-10}
	$= 0.64X(2p \rightarrow 3p)$	145	7.0×10^{-10}	6.5×10^{-10}
	$= 0.79X(2p \rightarrow 3p)$	210	7.7×10^{-10}	7.5×10^{-10}
	$X(2s \rightarrow 3d) = 0.30X(2p \rightarrow 3d)$	110	1.2×10^{-9}	1.5×10^{-9}
	$= 0.30X(2p \rightarrow 3d)$	145	1.3×10^{-9}	1.5×10^{-9}
	$= 0.29X(2p \rightarrow 3d)$	210	1.2×10^{-9}	1.5×10^{-9}

levels about 10%. The errors caused by collisional mixing of the upper levels will be about 10% for the $n = 3$ levels and less than 50% for the $n = 4$ levels.

For O VI the total error will be somewhat larger since O VI is a natural contaminant of relatively large concentrations in our plasmas. The uncertainty in the correction for optical depth is estimated to be less than 10% for the O VI values quoted. Other O VI values obtained with higher electron densities were omitted from the tables since the resonance line was influenced too strongly by self-absorption. Due to the large natural concentration of oxygen, the uncertainty in the oxygen concentration is somewhat larger and is estimated to 25%.

TABLE VII. Excitation-rate coefficients to $n = 4$ levels.

Ion	Rate Coefficient ($cm^3 sec^{-1}$)	T(eV)	Measured	Bely
Ne VIII	$X(2s \rightarrow 4s)$	125	3.7×10^{-11}	2.3×10^{-11}
		165	3.7×10^{-11}	2.8×10^{-11}
		260	3.5×10^{-11}	3.4×10^{-11}
	$X(2s \rightarrow 4p)$	125	2.5×10^{-11}	2.7×10^{-11}
		165	2.0×10^{-11}	3.7×10^{-11}
		260	3.5×10^{-11}	5.2×10^{-11}
	$X(2s \rightarrow 4d)$	125	3.5×10^{-11}	4.2×10^{-11}
		165	2.8×10^{-11}	5.3×10^{-11}
		260	4.0×10^{-11}	6.6×10^{-11}
O VI	$X(2s \rightarrow 4s)$	260	3.3×10^{-11}	7.5×10^{-11}
	$X(2s \rightarrow 4p) = X(2p \rightarrow 4p)$	260	5.2×10^{-11}	13×10^{-11}
	$X(2s \rightarrow 4d) = 0.32X(2p \rightarrow 4d)$	260	5.5×10^{-11}	16×10^{-11}
N V	$X(2s \rightarrow 4s)$	110	0.8×10^{-10}	1.2×10^{-10}
		145	1.1×10^{-10}	1.2×10^{-10}
		210	1.0×10^{-10}	1.2×10^{-10}
	$X(2s \rightarrow 4p) = 0.68X(2p \rightarrow 4p)$	110	0.63×10^{-10}	1.6×10^{-10}
	$= 0.78X(2p \rightarrow 4p)$	145	0.8×10^{-10}	1.9×10^{-10}
	$= 0.95X(2p \rightarrow 4p)$	210	0.9×10^{-10}	2.2×10^{-10}
	$X(2s \rightarrow 4d) = 0.33X(2p \rightarrow 4d)$	110	1.5×10^{-10}	2.4×10^{-10}
	$= 0.32X(2p \rightarrow 4d)$	145	1.5×10^{-10}	2.5×10^{-10}
	$= 0.31X(2p \rightarrow 4d)$	210	2.0×10^{-10}	2.6×10^{-10}

V. SUMMARY

Excitation-rate coefficients for lithiumlike ions are derived from absolute line intensities emitted by suitable ions in well-diagnosed plasmas. The results are compared with calculations using the Coulomb-Born approximation. The maximum experimental error of the individual rate coefficient is a factor of 2. However, the mean error will be smaller, and if one calculates the standard deviation of the experimental values from the theoretical ones averaged over N v, O vi, and Ne viii, one obtains a deviation of less than 30% for excitation to the $n = 2$ and $n = 3$ levels and less than 40% for excitation to the 4*s* level. The rates for excitation to the 4*p* and 4*d* levels, however, are consistently about 40% below the theoretical ones. This discrepancy cannot be caused by further excitation or ionization. The ionization rate is estimated,[24] for example, to be less than 3% of the radiative decay rate.

After completion of this work a paper by Boland *et al.*[37] appeared on measurements of excitation rates for N v. The technique used is essentially identical to the one employed in this paper. The experiments were done on a large plasma device known as ZETA, where the electron density is $\sim 10^{14}$ cm^{-3}. The excitation-rate coefficient is obtained for five transitions in N v at one temperature ($T_e = 20$ eV). The final results are also in agreement with the theory within the experimental uncertainty. Both experiments thus support the theoretical calculations obtained in the Coulomb-Born approximation.

ACKNOWLEDGMENTS

The authors would like to express their appreciation to H. R. Griem for valuable discussions. The computer time for this project was supported by the National Aeronautics and Space Administration Grant No. NSG-398 to the Computer Science Center of the University of Maryland. The National Science Foundation gave a grant for the purchase of the grazing-incidence spectrograph used in this work.

*Supported by the Atomic Energy Commission.

[1]L. Heroux, Nature 198, 1291 (1963).

[2]L. Heroux, Proc. Phys. Soc. (London) 83, 121 (1964).

[3]H. E. Hinteregger, L. A. Hall, and W. Schweizer, Astrophys. J. 140, 319 (1964).

[4]K. G. Widing and G. D. Sandlin, Astrophys. J. 152, 545 (1968).

[5]B. Boland, F. Jahoda, T. J. L. Jones, and R. W. P. McWhirter, in *Fourth International Conference on the Physics of Electronic and Atomic Collisions, Quebec*, 1965, edited by L. Kerwin and W. Fite (Science Bookcrafters, Hastings-on-Hudson, N. Y., 1965).

[6]E. Hinnov, J. Opt. Soc. Am. 56, 1179 (1966); 57, 1392 (1967).

[7]L. C. Johnson, Phys. Rev. 155, 64 (1967).

[8]R. C. Elton and W. W. Köppendörfer, Phys. Rev. 160, 194 (1967).

[9]H. -J. Kunze, A. H. Gabriel, and H. R. Griem, Phys. Rev. 165, 267 (1968).

[10]The assumption of a steady-state population for the excited states is justified in all practical cases. Characteristic times for changes in the excited-state densities are of the order of radiative lifetimes A^{-1}, see Ref. 9.

[11]M. J. Seaton, in *Atomic and Molecular Processes*, edited by D. R. Bates (Academic, New York, 1962), p. 414.

[12]H. Van Regemorter, Astrophys. J. 136, 906 (1962).

[13]C. W. Allen, *Astrophysical Quantities* (Athlone, University of London, London, 1963), 2nd ed.

[14]H. R. Griem, Phys. Rev. 165, 258 (1968).

[15]D. E. Roberts, *Sixth International Conference on the Physics of Electronic and Atomic Collisions, Cambridge, Mass., Abstracts of Papers* (MIT Press, Cambridge, Mass., 1969), p. 257.

[16]R. C. Elton, in *Methods of Experimental Physics - Plasma Physics*, edited by H. R. Griem and R. H. Lovberg (Academic, New York, 1970).

[17]P. G. Burke, J. H. Tait, and B. A. Lewis, Proc. Phys. Soc. (London) 87, 209 (1966).

[18]O. Bely, Proc. Phys. Soc. (London) 88, 587 (1966); Ann. Astrophys. 29, 131 (1966).

[19]O. Bely, Ann. Astrophys. 29, 683 (1966).

[20]O. Bely and D. Petrini, Astron. Astrophys. 6, 318 (1970).

[21]A. W. DeSilva and H. -J. Kunze, J. Appl. Phys. 39, 2458 (1968).

[22]H. -J. Kunze and A. H. Gabriel, Phys. Fluids 11, 1216 (1968).

[23]H. -J. Kunze, in *Plasma Diagnostics*, edited by Lochte-Holtgreven (North-Holland, Amsterdam, 1968).

[24]H. -J. Kunze, Phys. Rev. A 3, 937 (1971).

[25]W. C. Griffin and R. W. P. McWhirter, *Proceedings of the Conference on Optical Instruments and Techniques* (Chapman and Hall, London, 1962), p. 14.

[26]E. Hinnov and F. W. Hofmann, J. Opt. Soc. Am. 53, 1259 (1962).

[27]H. Magdeburg, Z. Naturforsch. 20a, 980 (1965).

[28]A. T. Hattenburg, Appl. Opt. 6, 95 (1967).

[29]W. L. Wiese, M. W. Smith, and B. M. Glennon, Natl. Bur. Std., Report No. NSRDS-NBS-4, Vol. 1, 1966 (unpublished).

[30]W. D. Johnston III and H. -J. Kunze, Astrophys. J. 157, 1469 (1969).

[31]J. L. Schwob, Ph.D. thesis, Faculte des Sciences de Paris, France, 1967 (unpublished).

[32]H. R. Griem, *Plasma Spectroscopy* (McGraw-Hill, New York, 1964).

[33]P. Kepple and H. R. Griem, Phys. Rev. 173, 317 (1968).

[34]We thank J. R. Greig for supplying the transmission curve for the Seya-Namioka monochromator. It was obtained by using two instruments in tandem.

[35]A. C. G. Mitchell and M. W. Zemansky, *Resonance Radiation and Excited Atoms* (Cambridge U.P., New York, 1961), Appendix V.

[36]B. Warner, Monthly Notices Roy. Astron. Soc. 141, 273 (1968).

[37]B. C. Boland, F. C. Jahoda, T. J. L. Jones, and R. W. P. McWhirter, J. Phys. B 3, 1134 (1970).